Exact Bit Error Rate Analysis of Ambient Backscatter Systems Under Fading Channels

J. Kartheek Devineni and Harpreet S. Dhillon

***Abstract*—The success of Internet-of-Things (IoT) relies on enabling the reliable exchange of data at low-rate and low-power among billions of battery-operated energy-constrained IoT devices. Ambient backscattering, with its technological capability of simultaneous information and energy transfer is quickly emerging as an appealing solution for this communication paradigm. In this paper, we investigate the detection of binary data transmitted using ambient backscatter at a receiver tracking the channel state information (CSI) of a flat-fading *Rayleigh* channel, and characterize the corresponding performance in terms of the bit-error probability. A binary hypothesis testing problem is formulated for the received signal and the performance of the receiver under *mean threshold (MT)* detection technique is analyzed. Two main contributions of the analysis that distinguish this work from the prior art are the characterization of the average signal energy in terms of the exact conditional density functions, and the characterization of average bit error rate (BER) expression for this setup. The key challenge lies in the handling of correlation between channel gains of two hypotheses for the derivation of joint probability distribution of magnitudes of channel gains that is needed for the BER analysis.**

***Index Terms*—Ambient backscattering, BER, Internet of Things, Hypothesis testing, Noncentral chi-squared distribution.**

I. Introduction

Internet of Things (IoT) is an exciting new paradigm where billions of inter-connected devices sense the physical world, exchange information and take appropriate decisions of everyday events with minimal human intervention. Two important aspects that are essential to enable this vision are the self-sustainability of the IoT devices and the periodic communication among these devices to exchange information. Ambient Backscatter is a promising new technology with the potential to support this low-power and low-rate communication to nearby devices. Ambient backscattering harvests energy from electromagnetic (EM) waves that are already present in the environment, like radio-frequency (RF) and television (TV) waves, and simultaneously backscatter data generated by modulating the reflected waves [1], [2].

The proof-of-concept systems related to the design of ambient backscatter have been developed in [1]–[5], which have demonstrated the feasibility of practical implementation of the technology. On the other hand, the investigation on theoretical aspects like throughput, error rates, and performance is still in nascent stages. Several important steps in this direction have been taken in [6]–[14] where BER analysis for ambient backscattering under different setups including different modulation schemes, non-coherent and semi-coherent detection, modulation over orthogonal frequency division multiplexing (OFDM) signals and receiver with multiple antennas, are investigated. The key enabler of the analysis in [6]–[14] is the approximation of average signal energy as Gaussian distributed. Despite this progress, the following two fundamental problems are still open for ambient backscatter systems: (i) the characterization of the exact distribution of average signal energy and (ii) the characterization of exact average BER in fading channels. Tackling these two problems is the main focus of this paper. Further details on the main contributions of the paper are presented next.

Contributions: We show that the exact conditional density functions of the average energy of the received signal follow noncentral chi-squared distribution (NC-χ^2). Characterization of the exact conditional signal distribution is an important component in the optimal performance analysis, which differentiates our work from the earlier works that approximated this distribution as Gaussian [6]–[9]. Using this result on conditional distributions, a binary hypothesis testing problem is formulated and the detection is performed by comparing the average energy of the signal to a threshold. In this paper, we focus on *mean threshold* detection in which the threshold is calculated as the mean of conditional expectations of the average signal energy received under different hypotheses. A key challenge in the error analysis is the need to characterize the joint distribution of correlated fading components belonging to the different hypotheses. In particular, although the individual links in the system may experience independent fading, overlapping backscatter data onto radio signals eventually results in different but correlated fading components for the two hypotheses. We derive the exact expression of this joint distribution function required for the average BER analysis. A key driver of this evaluation is the independence of fading component of the alternate hypothesis conditioned on fading component of the null hypothesis.

II. System Model

We consider a pair of devices, of which one is a backscatter transmitter (BTx) and the other is a receiver (Rx). We assume the presence of modulated carrier waves generated by a source in the environment, henceforth referred to as *ambient waves* and *ambient source* respectively, and the devices communicate through scattering of the incident ambient waves. This is a valid assumption since such sources of carrier waves, for example TV, cellular or Wi-Fi networks, are almost omnipresent.

J. K. Devineni and H. S. Dhillon are with Wireless@VT, Department of ECE, Virginia Tech, Blacksburg, VA (email: kartheekdj@vt.edu and hdhillon@vt.edu).

Backscatter derives its name from the mode of information exchange, which is to communicate data through reflection of RF waves, and the procedure of backscattering ambient RF waves is called *ambient backscatter*. To understand the operation of data modulation using backscatter, it is essential to look at the propagation of an electromagnetic (EM) wave between different surfaces. When EM waves received at an antenna propagate through load, part of the wave is reflected back into free space due to impedance mismatch between the antenna and the load component (which forms the main circuit) and is used for backscattering data. The load impedance typically is of a complex value and the reflection coefficient α at the boundary between antenna and load is given by [15]:

$$\alpha = \frac{\frac{Z_L}{Z_a^*} - 1}{\frac{Z_L}{Z_a} + 1}, \tag{1}$$

where Z_L and Z_a are the impedances of the load and antenna respectively and the symbol $*$ represents complex conjugate. In order to transfer all the power to load, the load impedance is set to $Z_L = Z_a^*$ which is known as *maximum power transfer* matching. On the other hand, in order to reflect all the power, the load impedance is set to $Z_L = 0$. Therefore, $Z_L = Z_a^*$ and $Z_L = 0$ are known as *non-reflecting* and *reflecting* states respectively. The backscatter system can leverage this to modulate data by tuning impedance of the load to vary reflection coefficient at this boundary. A simple modulation scheme is to tune the circuit between reflecting and non-reflecting states when transmitting bits 1 and 0, respectively. The system model for the ambient backscatter is illustrated in Fig. 1. The devices in the network are assumed to either have their own power source or generate enough power from the ambient waves to run their circuits. The latter assumption is valid mainly because the ambient backscatter systems are designed to operate at a very low power, of the order of few μWs.

A. Channel Model

In this paper, we assume that the backscatter transmitter and receiver are located in a rich scattering environment, for which flat Rayleigh fading channel is a prominent choice. Handling more general fading distributions is a useful direction of future work. In the backscatter setup illustrated in Fig. 1, there are two direct communication links, one each from *ambient source* to transmitter and receiver, and one backscatter communication link, from transmitter to receiver. The fading components of the direct links to receiver and transmitter, and the backscatter link are independent, identically distributed and are denoted by h_r, h_t and h_b, respectively. The average energy of the ambient signal is assumed to be unity and the variance σ^2 of zero mean complex additive Gaussian noise is varied to obtain different SNR values. For this reason, the exact units of signal energy are not needed and SNR is used as a measure of the signal strength in the distribution plots.

B. Signal Model

At the BTx, a simple binary on-off modulation scheme is implemented using reflecting and non-reflecting states to transmit digital bits. The desired signal at the Rx (shown in Fig. 1) is the sum of two components, one directly received from the *ambient source* and the other reflected from the BTx. The received signal of an ambient backscatter system is mathematically expressed as follows:

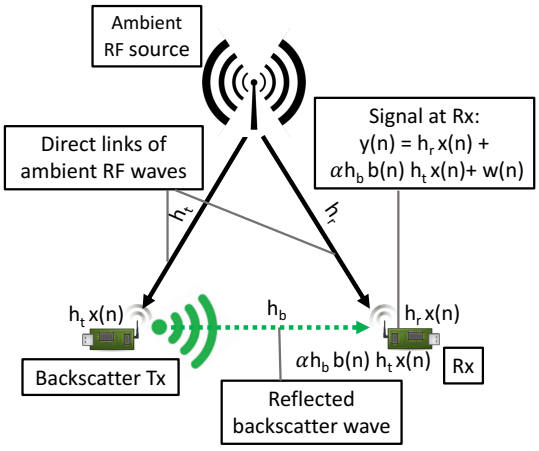

Fig. 1. System model of ambient backscatter communication system.

$$y(n) = \underbrace{h_r x(n)}_{\text{radio signal}} + \underbrace{\alpha h_b\, b(n)\, h_t x(n)}_{\text{backscatter signal}} + \underbrace{w(n)}_{\text{i.i.d Gaussian noise}}, \tag{2}$$

where $x(n)$ and $w(n)$ are complex baseband ambient radio and complex additive Gaussian noise signals respectively, $b(n) \in \{0, 1\}$ is the backscatter data and α is the reflection coefficient of the transmitter node at the boundary of antenna and circuit.

The radio signals will be carrying the ambient source data at a higher rate compared to the backscatter data. This simple fact can be exploited to separate backscatter data from ambient source data, which is achieved by averaging energy of finite samples of the received signal (given by length N) over which the backscatter data remains constant [1]. The average energy of $x(n)$ over a sample length N is assumed to be a constant given by:

$$\bar{E} = \frac{1}{N} \sum_{n=1}^{N} |x(n)|^2. \tag{3}$$

As $b(n)$ remains the same over sample length N, the model in (2) can be simplified, by taking $b(n) = b$, as follows:

$$y(n) = (h_r + \alpha h_b h_t b)\, x(n) + w(n), \quad (1 \le n \le N). \tag{4}$$

To further simplify the model, received signal $y(n)$ can be expressed separately for each value of bit b with the following fading components:

$$y(n) = \begin{cases} h_0\, x(n) + w(n), & b = 0, \\ h_1\, x(n) + w(n), & b = 1, \end{cases} \tag{5}$$

where $h_0 = h_r$ and $h_1 = h_r + \alpha h_b h_t$ are fading components dependent on backscatter data b. The magnitude square of the fading components are denoted by $\mu = |h_0|^2$ and $\nu = |h_1|^2$.

Remark 1. *It should be noted that the fading terms h_0 and h_1 (also μ and ν) are different and are correlated due to the common term h_r in their expressions, unlike a traditional BPSK system which has a single fading term.*

The receiver is assumed to track CSI which means that both h_0 and h_1 are known at the receiver. This assumption will be relaxed in the expanded version of the paper where detection without channel information will also be studied.

III. Signal Detection

A. Exact Distribution Functions

The BTx node will modulate its own data onto the reflected ambient radio waves which means that the Rx node has to implement a mechanism to separate backscatter data from the *ambient source* data. For this purpose, energy of the received signal is averaged over a window of N samples. This mechanism results in a random variable (RV) Y representing the average signal energy, and the operation is represented as follows [1]:

$$Y = \frac{1}{N}\sum_{n=1}^{N}|y(n)|^2 = \frac{1}{N}\sum_{n=1}^{N}|(h_r + \alpha h_b\ b\ h_t)x(n) + w(n)|^2. \tag{6}$$

This problem is formulated as a binary hypothesis testing problem where the scenarios conditioned on bits $b = 0$ and $b = 1$ are taken as $\mathcal{H}_0$ (Null Hypothesis) as $\mathcal{H}_1$ (Alternate Hypothesis) respectively:

$$\mathcal{H}_0 : Y = \frac{1}{N}\sum_{n=1}^{N}|h_0 x(n) + w(n)|^2, \qquad b = 0, \tag{7}$$

$$\mathcal{H}_1 : Y = \frac{1}{N}\sum_{n=1}^{N}|h_1 x(n) + w(n)|^2, \qquad b = 1. \tag{8}$$

The conditional probability density functions (PDFs) of Y are crucial in the detection and estimation of the transmitted bit and are derived in the following Lemma.

Lemma 1. *The PDF of Y conditioned on $\mathcal{H}_0$, μ and $\mathcal{H}_1$, ν are respectively given by:*

$$f_{Y|\mathcal{H}_0,\mu}(t) = \frac{2N}{\sigma^2}\sum_{i=0}^{\infty}\frac{e^{-\frac{\mu N\bar{E}}{\sigma^2}}\left(\frac{\mu N\bar{E}}{\sigma^2}\right)^i}{i!}f_{\chi^2}(\frac{2N}{\sigma^2}t; 2N+2i), \tag{9}$$

$$f_{Y|\mathcal{H}_1,\nu}(t) = \frac{2N}{\sigma^2}\sum_{i=0}^{\infty}\frac{e^{-\frac{\nu N\bar{E}}{\sigma^2}}\left(\frac{\nu N\bar{E}}{\sigma^2}\right)^i}{i!}f_{\chi^2}(\frac{2N}{\sigma^2}t; 2N+2i). \tag{10}$$

Proof: See Appendix A. ∎

Remark 2. *It can be observed that the PDFs of Y conditioned on $\mathcal{H}_0$ and $\mathcal{H}_1$ are respectively dependent only on parameters μ and ν, which are the squares of absolute values of the respective channel coefficients h_0 and h_1. Thus, the average BER can be written as the expectation of BER conditioned jointly (since they are not independent) on just μ and ν.*

B. Comparison with Approximate Distribution Functions

The exact conditional PDFs derived here are compared with the approximations available in the literature. An alternate

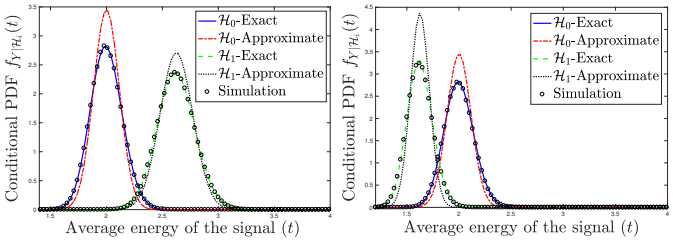

Fig. 2. Comparison of exact (derived in this paper) and approximate conditional PDFs [9] of average signal energy Y for $\mu = 1, \nu = 1.625$ (left) and $\mu = 1, \nu = 0.625$ (right) at SNR = 0 dB, $N = 150$.

representation of Y can be derived by expanding (6) and is given by the expression:

$$Y = \underbrace{|h_r + \alpha h_b h_t b|^2\bar{E}}_{\text{constant}} + \underbrace{\frac{1}{N}\sum_{n=1}^{N}|w(n)|^2}_{\text{Central-}\chi^2\text{ RV}} + \underbrace{\frac{2}{N}\,\text{Re}\left\{(h_r + \alpha h_b h_t b)\sum_{n=1}^{N}x(n)w^*(n)\right\}}_{\text{Gaussian RV}}, \tag{11}$$

The Gaussian approximation of Y can be made by approximating the Central-χ^2 RV with its mean value. This approximation is equivalent to the approximation given for a large value of N in [9], which is also the preferred mode of approximation in the referenced paper. The exact and approximated conditional PDFs of the average signal energy Y for N = 150 and SNR = 0 dB are compared in Fig. 2, and the deviation in the plots is clearly noticeable. The other approximated distributions, provided for a small value of N in [9], are also compared with our exact distributions, the results of which will be included in the extended version of the paper. As expected, the exact distributions derived in this paper match exactly with the simulated conditional PDFs. The impact of channel variations on the conditional PDFs is analyzed by plotting them for two sets of values of channel parameters μ and ν. When the two sub-plots in Fig. 2 are compared, the conditional distributions of two hypotheses are observed to interchange their positions which means that the relative positions of the conditional distributions of two hypotheses change with channel parameters μ and ν.

C. Detection Threshold

Due to space constraints, we focus on a simple detection strategy, which we term as MT detection. More complex threshold techniques including maximum likelihood (ML) detection will be analyzed in the expanded version. The threshold value of MT detection method is evaluated as the mean of the conditional expectations of average signal energy Y given $\mathcal{H}_0, \mu$ and $\mathcal{H}_1, \nu$:

$$T_{\text{mt}} = \frac{\mathbb{E}[Y|\mathcal{H}_0] + \mathbb{E}[Y|\mathcal{H}_1]}{2} = \sigma^2 + \frac{\bar{E}(\mu+\nu)}{2}. \tag{12}$$

IV. Bit Error Rate Analysis

As noted in Remark 2, average BER of an ambient backscatter system (ABS) is dependent on joint distribution of the

fading components μ and ν. The analytical expression of the average BER in a fading channel can be written as:

$$P_{e,\mathrm{ABS}} = \mathbb{E}_{\mu,\nu}[P(e|\mu,\nu)] \tag{13}$$

$$= \int_0^\infty \int_0^\infty f_{\mu,\nu}(\mu,\nu) P(e|\mu,\nu)\, \mathrm{d}\nu\, \mathrm{d}\mu, \tag{14}$$

where $f_{\mu,\nu}(\mu,\nu)$ is the joint probability density of fading components μ and ν, and $P(e|\mu,\nu)$ is the error probability conditioned on μ and ν. The expressions of the two components are derived next.

Lemma 2. *The joint density of the fading components μ and ν is given by the following expression:*

$$f_{\mu,\nu}(\mu,\nu) = \frac{1}{\pi\sigma_h^2} e^{-\frac{\mu}{\sigma_h^2}} \frac{1}{2\pi(|\alpha|\sigma_h^2)^2} \times \int_0^{2\pi}\int_0^{2\pi} K_0\Big(\frac{\sqrt{\mu+\nu-2\sqrt{\mu\nu}\cos(\theta_{h_1}-\theta_{h_0})}}{\frac{|\alpha|\sigma_h^2}{2}}\Big)\mathrm{d}\theta_{h_1}\mathrm{d}\theta_{h_0}, \tag{15}$$

where $K_0(z)$ is the zeroth order modified Bessel function of second kind.

Proof: See Appendix B. ∎

Theorem 1. *The ergodic BER for a receiver with CSI in an ambient backscatter system is:*

$$P_{e,\mathrm{ABS}} = \int_{\mu=0}^{\infty}\int_{\nu=0}^{\mu} f_{\mu,\nu}(\mu,\nu) \times \frac{1}{2}\Bigg(\int_0^{T(\mu,\nu)} f_{Y|\mathcal{H}_0,\mu}(t)\,\mathrm{d}t + \int_{T(\mu,\nu)}^{\infty} f_{Y|\mathcal{H}_1,\nu}(t)\,\mathrm{d}t\Bigg)\mathrm{d}\nu\,\mathrm{d}\mu + \int_{\mu=0}^{\infty}\int_{\nu=\mu}^{\infty} f_{\mu,\nu}(\mu,\nu)\times \frac{1}{2}\Bigg(\int_{T(\mu,\nu)}^{\infty} f_{Y|\mathcal{H}_0,\mu}(t)\,\mathrm{d}t + \int_0^{T(\mu,\nu)} f_{Y|\mathcal{H}_1,\nu}(t)\,\mathrm{d}t\Bigg)\mathrm{d}\nu\,\mathrm{d}\mu, \tag{16}$$

where the threshold $T(\mu,\nu)$ depends on the detection strategy.

Proof: The conditional error probability is given by:

$$P(e|\mu,\nu) = P(\mathcal{H}_0)P(e|\mathcal{H}_0,\mu) + P(\mathcal{H}_1)P(e|\mathcal{H}_1,\nu). \tag{17}$$

Assuming the symbols are equally likely, the prior probabilities of the two hypotheses are given by $P(\mathcal{H}_0) = P(\mathcal{H}_1) = \frac{1}{2}$. The conditional error probability of each hypothesis is given by the following relation since the relative values of μ,ν change the position of conditional distribution curves:

$$P(e|\mathcal{H}_0,\mu) = \begin{cases} \int_0^{T(\mu,\nu)} f_{Y|\mathcal{H}_0,\mu}(t)\,\mathrm{d}t, & \nu < \mu, \\ \int_{T(\mu,\nu)}^{\infty} f_{Y|\mathcal{H}_0,\mu}(t)\,\mathrm{d}t, & \nu \geq \mu. \end{cases} \tag{18}$$

$$P(e|\mathcal{H}_1,\nu) = \begin{cases} \int_{T(\mu,\nu)}^{\infty} f_{Y|\mathcal{H}_1,\nu}(t)\,\mathrm{d}t, & \nu < \mu, \\ \int_0^{T(\mu,\nu)} f_{Y|\mathcal{H}_1,\nu}(t)\,\mathrm{d}t, & \nu \geq \mu. \end{cases} \tag{19}$$

Partitioning the expression in (14) piecewise over the disjoint sets $\nu < \mu$ and $\nu \geq \mu$, and substituting the expressions of conditional error probability, we obtain the result. ∎

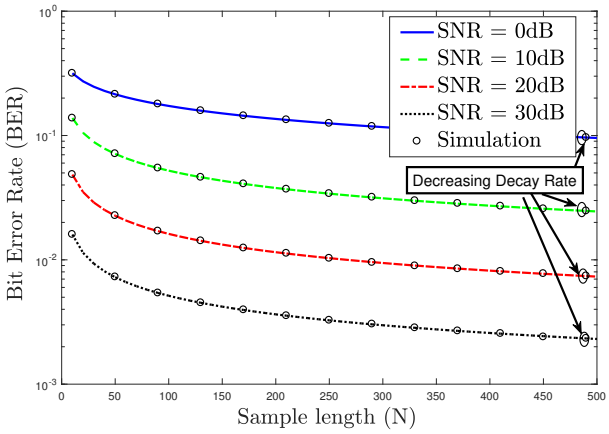

Fig. 3. BER versus N for different SNR values.

Remark 3. *Conditional error probabilities can be represented in terms of generalized Marcum Q-function as [16], [17] :*

$$P(e|\mu,\nu) = \begin{cases} \frac{1}{2}\Big\{1 + Q_N\Big(\sqrt{2N\frac{\mu\bar{E}}{\sigma^2}}, \sqrt{2N\frac{T(\mu,\nu)}{\sigma^2}}\Big) \\ \quad -Q_N\Big(\sqrt{2N\frac{\nu\bar{E}}{\sigma^2}}, \sqrt{2N\frac{T(\mu,\nu)}{\sigma^2}}\Big)\Big\} & \nu < \mu, \\ \frac{1}{2}\Big\{1 + Q_N\Big(\sqrt{2N\frac{\nu\bar{E}}{\sigma^2}}, \sqrt{2N\frac{T(\mu,\nu)}{\sigma^2}}\Big) \\ \quad -Q_N\Big(\sqrt{2N\frac{\mu\bar{E}}{\sigma^2}}, \sqrt{2N\frac{T(\mu,\nu)}{\sigma^2}}\Big)\Big\} & \nu \geq \mu. \end{cases} \tag{20}$$

We can observe from (20) *that the conditional BER expressions are functions of the parameters N, $\frac{\mu\bar{E}}{\sigma^2}$, $\frac{\nu\bar{E}}{\sigma^2}$ and $\frac{T(\mu,\nu)}{\sigma^2}$. The fraction $\frac{T(\mu,\nu)}{\sigma^2}$ of the MT threshold can be modified as:*

$$\frac{T_{\mathrm{mt}}}{\sigma^2} = 1 + \frac{\frac{\mu\bar{E}}{\sigma^2} + \frac{\nu\bar{E}}{\sigma^2}}{2}, \tag{21}$$

which is a function of the other three parameters N, $\frac{\mu\bar{E}}{\sigma^2}$ and $\frac{\nu\bar{E}}{\sigma^2}$. The fractions $\frac{\mu\bar{E}}{\sigma^2}$ and $\frac{\nu\bar{E}}{\sigma^2}$ are the received SNRs under the two hypotheses. Hence, it can be concluded that the BER of the system depends upon the signal and noise strength through SNR and not their respective energies separately.

V. Numerical Results and Discussion

In this section, we plot the analytical results derived in the previous section to glean system design insights. The analytical results are also validated by comparing with Monte Carlo simulations. The reflection coefficient α is set appropriately to approximate the 1.1 dB signal attenuation mentioned in [2] and the variance σ_h^2 of fading links is set to 1 for the system evaluation. With respect to any given system parameter, we refer to *decay rate* as the rate of decrement in BER with the increasing value of that parameter. In Fig. 3, we present the BER as a function of sample length N for different SNR values. It can be observed that the decay rate decreases with respect to N. A similar comparison is shown in Fig. 4 by plotting BER against SNR for different values of N. The gain

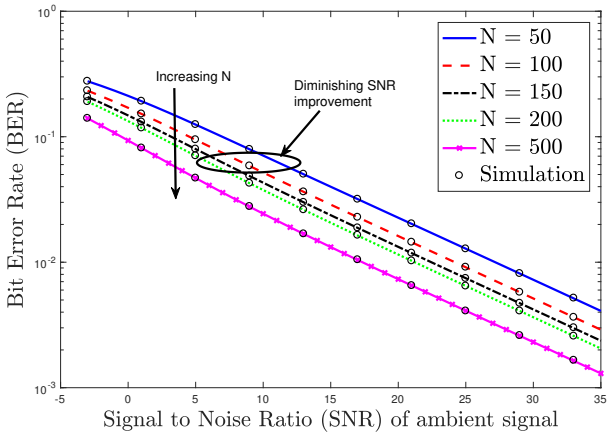

Fig. 4. BER versus SNR for different N values.

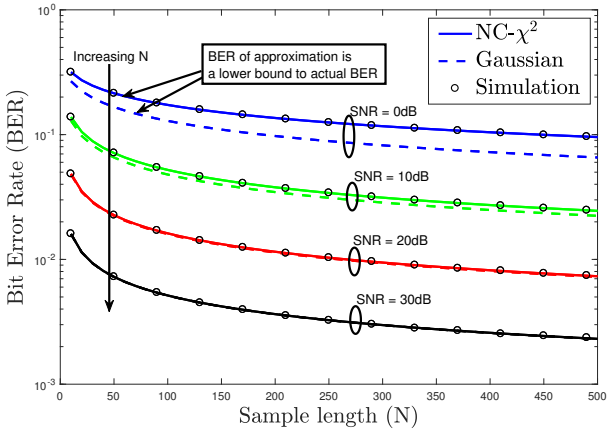

Fig. 5. BER under the actual and approximated distribution for different SNR.

in SNR of the system has diminishing returns with increasing N as the performance of the energy averaging operation at the receiver converges to a limit, thereby limiting the improvement in BER. The difference in BER accuracy when using the approximated distribution instead of the exact distribution is compared in Fig. 5. The preferred Gaussian approximation in [9], given for large N, does not result in accurate BER at the lower SNR range. The tightness of the approximation improves with increasing SNR.

VI. Conclusion

In this paper, the exact conditional distributions of the average energy of the received signal in ambient backscatter is characterized in terms of the noncentral chi-squared distribution. Further, the error performance of a receiver with CSI in a flat Rayleigh fading channel is analyzed by deriving the exact average BER expression for this system. The analytical evaluation of the joint distribution of correlated fading components is a key intermediate result of this analysis. Several key insights are drawn from the aforementioned analyses. First, BER of the ambient backscatter system is dependent on the energies of the signal and noise as a function of SNR of the signal and not separately on the individual energies, a trend similar to the one observed in standard BPSK modulation. Second, increasing the sample length N provides diminishing returns in terms of BER improvement.

Appendix

A. Proof of Lemma 1

The conditional PDF of Y under $\mathcal{H}_0$ can be obtained from the conditional PDF of a scaled version given by $Z = \frac{Y}{c}$, where $c = \frac{\sigma^2}{2N}$. The expression of Z can be written as follows:

$$Z = \frac{2}{\sigma^2}\sum_{n=1}^{N} |x(n)(h_r + h_b\alpha b h_t) + w(n)|^2. \tag{22}$$

Expanding $x(n) = x_r(n) + \mathrm{j}x_i(n)$, $h_0 = h_{0r} + \mathrm{j}h_{0i}$ and $w(n) = w_r(n) + \mathrm{j}w_i(n)$, where $\mathrm{j} = \sqrt{-1}$, results in the form:

$$\begin{aligned} Z &= \frac{2}{\sigma^2}\sum_{n=1}^{N} |(x_r(n) + \mathrm{j}x_i(n))(h_{0r} + \mathrm{j}h_{0i}) \\ &\qquad + w_r(n) + \mathrm{j}w_i(n)|^2, \\ &= \sum_{n=1}^{N} \frac{2}{\sigma^2}\left(x_r(n)h_{0r} - x_i(n)h_{0i} + w_r(n)\right)^2 \\ &\quad + \sum_{n=1}^{N} \frac{2}{\sigma^2}\left(x_r(n)h_{0i} + x_i(n)h_{0r} + w_i(n)\right)^2, \end{aligned} \tag{23}$$

where each term in the two summations is a square of an independent non-zero mean Gaussian RV with unit variance when conditioned on fading and $x(n)$. Also, notice that there are a total of $2N$ independent real-valued RVs.

The density function of this sum is given by noncentral chi-squared distribution [18]. This distribution is associated with a non-centrality parameter λ which is equal to the sum of the squared means of each Gaussian RV. The value of λ corresponding to Z can be evaluated as:

$$\begin{aligned} \lambda &= \frac{2\sum_{n=1}^{N}\left(x_r(n)h_{0r} - x_i(n)h_{0i}\right)^2}{\sigma^2} \\ &\qquad + \frac{2\sum_{n=1}^{N}\left(x_r(n)h_{0i} + x_i(n)h_{0r}\right)^2}{\sigma^2} \end{aligned} \tag{24}$$

$$= \frac{2\sum_{n=1}^{N}|x(n)|^2|h_0|^2}{\sigma^2} = \frac{2\sum_{n=1}^{N}|x(n)|^2\mu}{\sigma^2} \overset{(a)}{=} \frac{2N\bar{E}\mu}{\sigma^2}. \tag{25}$$

where (a) follows from the average energy given by (3).

Notice that the distribution of Z is independent of $x(n)$ since the parameter λ approaches a constant value because of (3). Therefore, the PDF of Z conditioned on $\mathcal{H}_0$ and μ is given by the noncentral chi-squared distribution with parameter λ calculated above:

$$\begin{aligned} f_{Z|\mathcal{H}_0,\mu}(z) &= \sum_{i=0}^{\infty} \frac{\exp(-\frac{\lambda}{2})(\frac{\lambda}{2})^i}{i!} f_{\chi^2}(z; 2N + 2i) \\ &= \sum_{i=0}^{\infty} \frac{\exp(-\frac{\mu N\bar{E}}{\sigma^2})(\frac{\mu N\bar{E}}{\sigma^2})^i}{i!} f_{\chi^2}(z; 2N + 2i), \end{aligned} \tag{26}$$

The conditional PDF $f_{Y|\mathcal{H}_0,\mu}(t)$ follows from the distribution of scaled transformation of a RV. The conditional PDF of Y under $\mathcal{H}_1$ is derived using similar procedure and is skipped.

B. Proof of Lemma 2

The distribution of independent and identical fading terms h_r, h_t and h_b is given by $\mathcal{CN}(0, \sigma_h^2)$. The distribution of $\alpha h_b \sim \mathcal{CN}(0, |\alpha|^2\sigma_h^2)$, formed by combining α and h_b, follows from the scalar multiplication property of circularly symmetric Gaussian random vectors [19].

The joint distribution of the real and imaginary parts of fading component h_0 is given by the Gaussian distribution. Similarly, the joint distribution of the real and imaginary parts of double Gaussian term $U = \alpha h_b h_t$ of the fading component h_1 is given in [20], [21]. For completeness, the expressions are provided below:

$$f_{h_{0R},h_{0I}}(h_{0r}, h_{0i}) = \frac{1}{\pi\sigma_h^2} \exp\left(-\frac{h_{0r}^2 + h_{0i}^2}{\sigma_h^2}\right), \tag{27}$$

$$f_{U_R,U_I}(u_r, u_i) = \frac{1}{2\pi\left(\frac{|\alpha|\sigma_h^2}{2}\right)^2} K_0\left(\frac{\sqrt{u_r^2 + u_i^2}}{\frac{|\alpha|\sigma_h^2}{2}}\right), \tag{28}$$

where K_0 is the zeroth order modified Bessel function of second kind.

The joint distribution of the real and imaginary parts of h_1 conditioned on h_0 is related to the joint distribution of U by the shift transformation property of a RV:

$$f_{h_{1R},h_{1I}|h_{0R},h_{0I}}(h_{1r}, h_{1i}) = f_{U_R,U_I}(h_{1r} - h_{0r}, h_{1i} - h_{0i}). \tag{29}$$

The joint distribution of the polar coordinates of h_0 and h_1 is derived from rectangular coordinates using the transformation property of RVs as follows:

$$\begin{aligned}
&f_{R_{h_0},\Theta_{h_0},R_{h_1},\Theta_{h_1}}(r_{h_0}, \theta_{h_0}, r_{h_1}, \theta_{h_1}) \\
&\overset{(h)}{=} f_{R_{h_0},\Theta_{h_0}}(r_{h_0}, \theta_{h_0})\ f_{R_{h_1},\Theta_{h1}|R_{h_0},\Theta_{h_0}}(r_{h_1}, \theta_{h_1}|r_{h_0}, \theta_{h_0}) \\
&\overset{(i)}{=} r_{h_0}\ f_{h_{0R},h_{0I}}(r_{h_0}\cos\theta_{h_0}, r_{h_0}\sin\theta_{h_0})\ r_{h_1} \times \\
&f_{U_R,U_I}(r_{h_1}\cos\theta_{h_1} - r_{h_0}\cos\theta_{h_0} r_{h_1}\sin\theta_{h_1} - r_{h_0}\sin\theta_{h_0}) \\
&= r_{h_0}\ \frac{1}{\pi\sigma_h^2} e^{-\frac{r_{h_0}^2}{\sigma_h^2}}\ r_{h_1}\ \frac{1}{2\pi\left(\frac{|\alpha|\sigma_h^2}{2}\right)^2} \times \\
&K_0\left(\frac{\sqrt{r_{h_1}^2 + r_{h_0}^2 - 2r_{h_1}r_{h_0}\cos(\theta_{h_1} - \theta_{h_0})}}{\frac{|\alpha|\sigma_h^2}{2}}\right),
\end{aligned} \tag{31}$$

where (h) follows from de-conditioning of RVs through chain rule and (i) follows from the relationship between the joint distribution functions of polar and rectangular coordinates.

The joint marginal distribution of R_{h_1}, R_{h_0}, obtained by integrating over the ranges of Θ_{h_0} and Θ_{h_1}, is given by:

$$\begin{aligned}
f_{R_{h_0},R_{h_1}}(r_{h_0}, r_{h_1}) = \int_0^{2\pi}\int_0^{2\pi} \frac{r_{h_0}}{\pi\sigma_h^2} e^{-\frac{r_{h_0}^2}{\sigma_h^2}} \frac{r_{h_1}}{2\pi\left(\frac{|\alpha|\sigma_h^2}{2}\right)^2} \times \\
K_0\left(\frac{\sqrt{r_{h_1}^2 + r_{h_0}^2 - 2r_{h_1}r_{h_0}\cos(\theta_{h_1} - \theta_{h_0})}}{\frac{|\alpha|\sigma_h^2}{2}}\right) \mathrm{d}\theta_{h_1}\mathrm{d}\theta_{h_0}.
\end{aligned} \tag{32}$$

Finally, the joint distribution of μ and ν is given by:

$$\begin{aligned}
&f_{\mu,\nu}(\mu, \nu) \overset{(j)}{=} \frac{1}{4\sqrt{\mu\nu}} f_{R_{h_0},R_{h_1}}(\sqrt{\mu}, \sqrt{\nu}) \\
&= \frac{1}{\pi\sigma_h^2} e^{-\frac{\mu}{\sigma_h^2}} \frac{1}{2\pi(|\alpha|\sigma_h^2)^2} \int_0^{2\pi}\int_0^{2\pi} \times \\
&K_0\left(\frac{\sqrt{\mu + \nu - 2\sqrt{\mu\nu}\cos(\theta_{h_1} - \theta_{h_0})}}{\frac{|\alpha|\sigma_h^2}{2}}\right) \mathrm{d}\theta_{h_1}\mathrm{d}\theta_{h_0},
\end{aligned} \tag{33}$$

where (j) follows from the relation between the joint PDFs of modulus of RVs given by R_{h_0} and R_{h_1}, and the square of modulus of the same RVs given by μ and ν, respectively.

REFERENCES

[1] V. Liu, A. Parks, V. Talla, S. Gollakota, D. Wetherall, and J. R. Smith, "Ambient backscatter: Wireless communication out of thin air," *Proc., ACM SIGCOMM*, Aug. 2013.

[2] B. Kellogg, V. Talla, S. Gollakota, and J. R. Smith, "Ambient backscatter: Wireless communication out of thin air," *Symposium on Networked Systems Design and Implementation (NSDI)*, Mar. 2016.

[3] B. Kellogg, A. Parks, S. Gollakota, J. R. Smith, and D. Wetherall, "Wi-Fi backscatter: Internet connectivity for RF-powered devices," *Proc., ACM SIGCOMM*, pp. 1–12, Aug. 2014.

[4] D. Bharadia, K. Joshi, M. Kotaru, and S. Katti, "BackFi: high throughput Wi-Fi backscatter," *Proc., ACM SIGCOMM*, pp. 283–296, Aug. 2015.

[5] V. Iyer, V. Talla, B. Kellogg, S. Gollakota, and J. R. Smith, "Inter-technology backscatter: towards internet connectivity for implanted devices," *Proc., ACM SIGCOMM*, pp. 1–14, Aug. 2016.

[6] G. Wang, F. Gao, Z. Dou, and C. Tellambura, "Uplink detection and BER analysis for ambient backscatter communication systems," *Proc., IEEE Globecom*, Dec. 2015.

[7] K. Lu, G. Wang, F. Qu, and Z. Zhong, "Signal detection and BER analysis for RF-powered devices utilizing ambient backscatter," *Proc., Intl. Conf. on Wireless Commun. & Sig. Proc. (WCSP)*, Oct. 2015.

[8] Y. Liu, Z. Zhong, G. Wang, and D. Hu, "Uplink detection and BER performance for wireless communication systems with ambient backscatter and multiple receiving antennas," *Proc., Intl. Conf. on Commun. and Networking in China (ChinaCom)*, pp. 79 – 84, Aug. 2015.

[9] G. Wang, F. Gao, R. Fan, and C. Tellambura, "Ambient backscatter communication systems: Detection and performance analysis," *IEEE Trans. on Commun.*, vol. 64, no. 11, pp. 4836 – 4846, Nov. 2016.

[10] Y. Liu, G. Wang, Z. Dou, and Z. Zhong, "New Coding and Detection Schemes for Ambient Backscatter Communication Systems," *IEEE Access*, Mar. 2017.

[11] J. Qian, F. Gao, G. Wang, S. Jin, and H. Zhu, "Semi-Coherent Detection and Performance Analysis for Ambient Backscatter System," *IEEE Trans. on Commun.*, vol. 65, no. 12, Dec. 2017.

[12] ——, "Noncoherent Detections for Ambient Backscatter System," *IEEE Trans. on Wireless Commun.*, vol. 16, no. 3, Mar. 2017.

[13] T. Zeng, G. Wang, Y. Wang, Z. Zhong, and C. Tellambura, "Statistical Covariance Based Signal Detection for Ambient Backscatter Communication Systems," *Proc., IEEE Veh. Technology Conf. (VTC)*, Sep. 2016.

[14] G. Yang, Y.-C. Liang, and Y. P. Rui Zhang, "Modulation in the Air: Backscatter Communication over Ambient OFDM Carrier," *IEEE Trans. on Commun.*, vol. 66, no. 3, Mar. 2018.

[15] K. Kurokawa, "Power waves and the scattering matrix," *IEEE Trans. on Microw. Theory and Tech.*, vol. MTT-13, no. 3, Mar. 1965.

[16] R. T. Short, "Computation of Rice and Noncentral Chi-Squared probabilities," *PhaseLocked Systems, Technical Report PHS0254*, Apr. 2012.

[17] D. A. Shnidman, "The calculation of the probability of detection and the Generalized Marcum Q-function," *IEEE Trans. on Info. Theory*, vol. 35, no. 2, Mar. 1989.

[18] M. Abramowitz and I. A. Stegun, "Handbook of mathematical functions," *Appl. Math. Ser. 55, National Bureau of Standards*, pp. 942–943, Jun. 1964.

[19] R. G. Gallager, "Circularly symmetric Gaussian random vectors," Jan. 2008.

[20] A. Papoulis, "Probability random variables and stochastic processes," *McGraw-Hill, 1st ed., p. 201*, 1965.

[21] N. O'Donoughue and J. M. F. Moura, "On the product of independent complex Gaussians," *IEEE Trans. on Signal Processing*, vol. 60, no. 3, Mar. 2012.